First-order correction terms in the weak-field asymptotic theory of tunneling ionization

Vinh H. Trinh,[1] Oleg I. Tolstikhin,[2,3] Lars Bojer Madsen,[4] and Toru Morishita[1]

[1]*Department of Engineering Science, The University of Electro-Communications, 1-5-1 Chofu-ga-oka, Chofu-shi, Tokyo 182-8585, Japan*

[2]*National Research Center "Kurchatov Institute," Kurchatov Square 1, Moscow 123182, Russia*

[3]*Moscow Institute of Physics and Technology, Dolgoprudny 141700, Russia*

[4]*Department of Physics and Astronomy, Aarhus University, 8000 Aarhus C, Denmark*

(Received 14 March 2013; published 26 April 2013)

The weak-field asymptotic theory (WFAT) of tunneling ionization in a static electric field is developed to the next order in field. The first-order corrections to the ionization rate and transverse momentum distribution of the ionized electrons are derived. This extends the region of applicability of the WFAT at the quantitative level toward stronger fields, practically up to the boundary between tunneling and over-the-barrier regimes of ionization. The results apply to any atom or molecule treated in the single-active-electron and frozen-nuclei approximations. The theory is illustrated by calculations for hydrogen and noble-gas atoms.

DOI: 10.1103/PhysRevA.87.043426 PACS number(s): 32.80.Rm, 33.80.Rv, 42.50.Hz

I. INTRODUCTION

Tunneling ionization is the first step for a variety of processes launched by the interaction of atoms and molecules with intense low-frequency few-cycle laser pulses [1,2]. Accurate ionization rates are required for the analysis of experimentally observable spectra of photoelectrons and ions [3–9] and harmonics [5,10–12] produced in such processes.

In the adiabatic regime, that is, for sufficiently low frequency at a given intensity, the interaction of an atom or molecule with an *oscillating* laser field can be described in terms of the outgoing-wave solution to the stationary Schrödinger equation which originates from the initial bound state in the presence of a *static* electric field [13]. Such solutions are called Siegert states (SSs) in an electric field [14,15]. In particular, the instantaneous value of the ionization rate is determined by the imaginary part of the complex SS energy eigenvalue as a function of the instantaneous value of field. Thus, the problem of calculating the ionization rate in a laser field reduces to that in a static electric field. The conditions of validity of the adiabatic approximation can be found in Ref. [13]. We note that for few-cycle laser pulses of current experimental interest the very concept of an ionization rate only has a meaning in the adiabatic regime.

Recently we have initiated the development of the weak-field asymptotic theory (WFAT) of tunneling ionization in a static electric field [16]. This theory generalizes the well-known results for hydrogen [17–19] and an arbitrary atom [20] and enables one to evaluate the ionization rate for an arbitrary molecule under the following approximations. The first is the single-active-electron approximation; extending the WFAT to many-electron systems becomes a priority goal for future studies. The second is the frozen-nuclei approximation; how to incorporate into the WFAT the effect of nuclear motion in molecules was shown in Ref. [21]. Finally, the third approximation, which gives the name of the theory, consists of the assumption that the ionizing field F is much less than a critical field F_c giving a boundary between tunneling and over-the-barrier regimes of ionization. In other words, the WFAT applies in the deep tunneling regime. In this case, the SS mentioned above can be constructed analytically and the ionization rate can be obtained as an asymptotic expansion in F. For neutral atoms and molecules in the ground state $F_c \sim 0.1$ a.u., which corresponds to an intensity $I \sim 3.5 \times 10^{14}$ W/cm^2. Thus, in spite of a seeming contradiction in terminology, the WFAT has a wide range of applications in modern strong-field physics.

In the leading-order approximation of the WFAT developed in Ref. [16], the ionization rate is given by a product of two factors which are now called *structure* and *field* factors [22,23]. The structure factor does not depend on F and is determined by the asymptotic tail of the unperturbed active electron's orbital. For atoms, because of spherical symmetry, it is just a number, but for molecules it is a function of the orientation with respect to the field which reveals valuable structure information. The structure factor presents one of the basic properties of atoms and molecules along with other related properties, such as dipole moment and polarizability. The techniques to calculate the molecular structure factors for a given orbital based on various quantum chemistry codes within the Hartree-Fock approximation were developed in Refs. [22,23]. The field factor, on the other hand, is a simple analytic function of F and the energy of the unperturbed orbital which does not depend on the orientation. While Refs. [22,23] were concerned with application of the leading-order WFAT to linear molecules, an application to nonlinear systems was demonstrated in Ref. [3] by the analysis of experimental photoelectron spectra of C_2H_4.

In the present work we develop the WFAT to the next order in field. So far, such an extension of the theory was available only for the hydrogen atom. In Ref. [24], the first-order correction to the leading-order term [18,19] in the weak-field asymptotics of the ionization rate of hydrogen in an arbitrary state was derived. In Ref. [25], a procedure to obtain higher-order terms in the asymptotic expansion was developed and a number of such terms for a few lowest states were given. In the case of the Coulomb potential, one can separate variables in the Schrödinger equation in parabolic coordinates, which crucially simplifies the analysis. This important advantage of parabolic coordinates is inherited in the general approach of Ref. [16], which applies to arbitrary one-electron potentials. This approach enables us to overcome technical difficulties and generalize the results of Ref. [24] to arbitrary atoms and molecules. We obtain the first-order correction terms in the

asymptotic expansions not only for the ionization rate, but also for the transverse momentum distribution (TMD) of the ionized electrons, which defines the photoelectron momentum distribution within the adiabatic theory [13]. These results essentially extend the region of applicability of the WFAT at the quantitative level toward stronger fields, practically up to $F \sim F_c$. Such an extension is the main goal of the present development.

The paper is organized as follows. In Sec. II, we summarize basic equations of the theory of SSs in an electric field [16]. In Sec. III, following the approach developed in Ref. [16], we construct the asymptotic solution of the SS eigenvalue problem for $F \to 0$, extending the results to the next order in F. The most technically involved part of the derivation is deferred to Appendix A. In Sec. IV, we present illustrative numerical results for hydrogen and noble-gas atoms. The WFAT results are compared with accurate numerical calculations by an original multiple-precision procedure outlined in Appendix B, for H, and by the method developed in Ref. [14], for Ne, Ar, Kr, and Xe. A summary of the results and the conclusions are given in Sec. V.

II. SIEGERT STATES IN AN ELECTRIC FIELD: BASIC EQUATIONS

We consider a molecule (for definiteness, we talk about molecules, but our analysis applies also to atoms) treated in the single-active-electron and frozen-nuclei approximations interacting with an external static uniform electric field $\mathbf{F} = F\mathbf{e}_z$, $F \geqslant 0$. The stationary Schrödinger equation for the active electron reads (atomic units are used throughout)

$$\left[-\tfrac{1}{2}\Delta + V(\mathbf{r}) + Fz - E\right]\psi(\mathbf{r}) = 0, \tag{1}$$

where $V(\mathbf{r})$ describes the interaction with the molecular ion and $\mathbf{r}$ is measured from the center of mass of the nuclei [16]. The potential $V(\mathbf{r})$ implicitly depends on the nuclear configuration and orientation of the molecule with respect to the field. It can be arbitrary, the only assumption is

$$V(\mathbf{r})|_{r\to\infty} = -\frac{Z}{r} - \frac{\mathbf{Dn}}{r^2} + O(r^{-3}), \tag{2}$$

where Z is the total charge of the molecular ion, $\mathbf{D}$ is its dipole moment, and $\mathbf{n} = \mathbf{r}/r$. The SSs are the solutions to Eq. (1) satisfying the regularity and outgoing-wave boundary conditions. To treat such solutions, it is convenient to introduce parabolic coordinates [17],

$$\xi = r + z, \qquad 0 \leqslant \xi < \infty, \tag{3a}$$

$$\eta = r - z, \qquad 0 \leqslant \eta < \infty, \tag{3b}$$

$$\varphi = \arctan\frac{y}{x}, \qquad 0 \leqslant \varphi < 2\pi, \tag{3c}$$

and rewrite Eq. (1) in the form [16]

$$\left[\frac{\partial}{\partial\eta}\eta\frac{\partial}{\partial\eta} + \mathcal{B}(\eta) + \frac{E\eta}{2} + \frac{F\eta^2}{4}\right]\psi(\mathbf{r}) = 0, \tag{4}$$

where the adiabatic Hamiltonian

$$\mathcal{B}(\eta) = \frac{\partial}{\partial\xi}\xi\frac{\partial}{\partial\xi} + \frac{\xi+\eta}{4\xi\eta}\frac{\partial^2}{\partial\varphi^2} - rV(\mathbf{r}) + \frac{E\xi}{2} - \frac{F\xi^2}{4} \tag{5}$$

is an operator acting on functions of ξ and φ and depending on η as a parameter. From Eq. (2) we obtain

$$\mathcal{B} \equiv \mathcal{B}(\eta)|_{\eta\to\infty} = \frac{\partial}{\partial\xi}\xi\frac{\partial}{\partial\xi} + \frac{1}{4\xi}\frac{\partial^2}{\partial\varphi^2} + Z + \frac{E\xi}{2} - \frac{F\xi^2}{4}. \tag{6}$$

In Ref. [16], the solution to Eq. (4) was sought as an expansion in terms of the *adiabatic* basis consisting of the eigenfunctions of $\mathcal{B}(\eta)$. Such an approach is indeed very efficient for numerical solution of the problem [14,15]. However, in the present analysis it is more convenient to use a *diabatic* basis consisting of the eigenfunctions of $\mathcal{B}$ defined by the equation

$$(\mathcal{B} - \beta_\nu)\Phi_\nu(\xi,\varphi) = 0 \tag{7}$$

supplemented by the regularity boundary condition at $\xi = 0$, zero boundary condition at $\xi \to \infty$, and periodic boundary condition in φ. Here ν is a discrete multi-index enumerating the solutions. Equation (7) allows separation of variables and has solutions of the form

$$\Phi_\nu(\xi,\varphi) = \phi_\nu(\xi)\frac{e^{im\varphi}}{\sqrt{2\pi}}, \tag{8a}$$

$$\nu = (n_\xi, m), \quad n_\xi = 0,1,\ldots, \quad m = 0, \pm 1, \ldots, \tag{8b}$$

where $\phi_\nu(\xi)$ and the corresponding eigenvalue β_ν are defined by

$$\left[\frac{d}{d\xi}\xi\frac{d}{d\xi} - \frac{m^2}{4\xi} + Z + \frac{E\xi}{2} - \frac{F\xi^2}{4} - \beta_\nu\right]\phi_\nu(\xi) = 0, \tag{9a}$$

$$\phi_\nu(\xi)|_{\xi\to 0} \propto \xi^{|m|/2}, \quad \phi_\nu(\xi)|_{\xi\to\infty} = 0, \tag{9b}$$

$$\int_0^\infty \phi_{n_\xi m}(\xi)\phi_{n'_\xi m}(\xi)\,d\xi = \delta_{n_\xi n'_\xi}. \tag{9c}$$

Here m is the azimuthal quantum number and n_ξ enumerates the different solutions to Eq. (9a) for a given m. The eigenfunctions (8a) are called parabolic channel functions. They are orthonormal with respect to the inner product

$$\langle\Phi_\nu|\Phi_{\nu'}\rangle \equiv \int_0^\infty\int_0^{2\pi}\phi_{n_\xi m}(\xi)\phi_{n'_\xi m'}(\xi)\frac{e^{i(m'-m)\varphi}}{2\pi}d\xi\,d\varphi = \delta_{\nu\nu'}, \tag{10}$$

where $\nu' = (n'_\xi, m')$. The solution to Eq. (4) is sought in the form

$$\psi(\mathbf{r}) = \eta^{-1/2}\sum_\nu f_\nu(\eta)\Phi_\nu(\xi,\varphi). \tag{11}$$

Substituting this expansion into Eq. (4), we obtain a set of ordinary differential equations defining the unknown functions $f_\nu(\eta)$,

$$\left[\frac{d^2}{d\eta^2} + \frac{F\eta}{4} + \frac{E}{2} + \frac{\beta_\nu}{\eta} + \frac{1-m^2}{4\eta^2}\right]f_\nu(\eta) - \frac{1}{\eta}\sum_{\nu'}W_{\nu\nu'}(\eta)f_{\nu'}(\eta) = 0, \tag{12}$$

where

$$W_{\nu\nu'}(\eta) = \langle\Phi_\nu\,|[rV(\mathbf{r}) + Z]|\,\Phi_{\nu'}\rangle. \tag{13}$$

The field term in Eq. (1) drives ionized electrons toward $z \to -\infty$, which corresponds to $\eta \to \infty$ [see Eq. (3b)]. This asymptotic region plays a key role in our analysis. The main advantage of parabolic coordinates in treating the SSs stems from the fact that Eqs. (12) become decoupled in this region. Indeed, from Eq. (2) we have

$$[rV(\mathbf{r}) + Z]|_{\eta\to\infty} = \frac{2D_z}{\eta} - 2(e^{-i\varphi}D_+ + e^{i\varphi}D_-)\frac{\xi^{1/2}}{\eta^{3/2}} + O(\eta^{-2}), \tag{14}$$

where $D_\pm = D_x \pm i\,D_y$. Thus the coupling matrix (13) vanishes at $\eta \to \infty$ and Eqs. (12) take the form

$$\left[\frac{d^2}{d\eta^2} + \frac{F\eta}{4} + \frac{E}{2} + \frac{\beta_\nu}{\eta} + \frac{\gamma_m}{\eta^2} + O(\eta^{-5/2})\right] f_\nu(\eta) = 0, \tag{15}$$

where

$$\gamma_m = \frac{1-m^2}{4} - 2D_z. \tag{16}$$

In Ref. [16], we retained only terms up to order $O(\eta^{-1})$ in this equation; this was sufficient for obtaining the leading-order term in the asymptotic solution of the problem for $F \to 0$. For deriving the first-order correction in F, we need terms up to order $O(\eta^{-2})$ in Eq. (15). The dominant contribution to the off-diagonal elements of $W_{\nu\nu'}(\eta)$ at $\eta \to \infty$, which couple the different parabolic channels, comes from the second term in the expansion (14). These coupling terms are represented by $O(\eta^{-5/2})$ in Eq. (15); their explicit form is immaterial for the following discussion. It is fortunate that they vanish faster than the term $O(\eta^{-2})$ needed for the present derivation, which greatly simplifies our analysis. It is convenient to introduce a boundary of the *coupling* or *core* region η_c such that for $\eta > \eta_c$ the last term in Eq. (15) can be neglected within a desired accuracy, and hence these equations for the different ν become decoupled. In the following, we consider only the region $\eta > \eta_c$. The outgoing-wave solution to Eq. (15) satisfies [16]

$$f_\nu(\eta)|_{\eta\to\infty} = \frac{2^{1/2} f_\nu}{(F\eta)^{1/4}} \exp\left[\frac{iF^{1/2}\eta^{3/2}}{3} + \frac{iE\eta^{1/2}}{F^{1/2}}\right]. \tag{17}$$

The solutions to Eqs. (12) satisfying the regularity boundary condition at $\eta = 0$ and the outgoing-wave boundary condition (17) at $\eta \to \infty$ exist only for a discrete set of generally complex values of E—this is the SS eigenvalue problem. The real and imaginary parts of the eigenvalue E define the energy $\mathcal{E}$ and ionization rate Γ of the state,

$$E = \mathcal{E} - \tfrac{i}{2}\,\Gamma. \tag{18}$$

The eigenfunction is normalized by

$$\int \psi^2(\mathbf{r})\,d\mathbf{r} = \frac{1}{4}\int_0^\infty\int_0^\infty\int_0^{2\pi} \psi^2(\mathbf{r})(\xi+\eta)d\xi\,d\eta\,d\varphi = 1, \tag{19}$$

where the integral should be regularized by deforming the integration path in η from the real semiaxis into a contour in the complex η plane (for more details see Ref. [14]).

The outgoing-wave boundary condition for Eq. (1) can also be presented in the form [16]

$$\psi(\mathbf{r})|_{z\to-\infty} = \int A(\mathbf{k}_\perp) e^{i\mathbf{k}_\perp\cdot\mathbf{r}_\perp} g(z,k_\perp)\,\frac{d\mathbf{k}_\perp}{(2\pi)^2}, \tag{20}$$

where $\mathbf{r}_\perp = (x,y) = (r_\perp\cos\varphi, r_\perp\sin\varphi)$, $\mathbf{k}_\perp = (k_x,k_y) = (k_\perp\cos\varphi_k, k_\perp\sin\varphi_k)$, and

$$g(z,k_\perp) = e^{-i\pi/12}2\pi^{1/2}(2F)^{-1/6}\,\mathrm{Ai}(\zeta), \tag{21a}$$

$$\zeta = \frac{2e^{-i\pi/3}}{(2F)^{2/3}}\left[E - Fz - \frac{k_\perp^2}{2}\right]. \tag{21b}$$

Here $\mathrm{Ai}(x)$ is the Airy function [26]. The function $g(z,k_\perp)$ contains only an outgoing wave as $z \to -\infty$. The TMD amplitude $A(\mathbf{k}_\perp)$ can be expressed in terms of the coefficients in Eq. (17) and parabolic channel functions (8) [16],

$$A(\mathbf{k}_\perp) = \frac{2^{3/2}\pi i}{F^{1/2}}\sum_\nu f_\nu \Phi_\nu\left(\frac{k_\perp^2}{F}, \varphi_k\right). \tag{22}$$

The TMD of ionized electrons in the outgoing flux is given by

$$P(\mathbf{k}_\perp) = |A(\mathbf{k}_\perp)|^2. \tag{23}$$

Thus the main quantities characterizing a SS and related to observables are the complex eigenvalue E defining its energy and ionization rate, Eq. (18), and the asymptotic coefficients f_ν in Eq. (17) defining the TMD amplitude (22). An efficient numerical procedure to accurately calculate E and f_ν was developed in Ref. [14], for axially symmetric potentials, and in Ref. [15], for arbitrary potentials without any symmetry.

III. WEAK-FIELD ASYMPTOTICS

Meanwhile, in the weak-field limit the values of E and f_ν can be found analytically. In Ref. [16], the leading-order asymptotic solution to the SS eigenvalue problem for

$$F \to 0 \tag{24}$$

was obtained. In this section, we derive the first-order correction to this solution. We follow the approach of Ref. [16], successively extending each of its steps to the next order in F.

A. Perturbation theory

Let, for $F = 0$, Eq. (1) have a bound-state solution with energy $E_0 < 0$ and wave function $\psi_0(\mathbf{r})$. It is convenient to introduce the notation

$$\varkappa = \sqrt{-2E_0}. \tag{25}$$

We assume that $\psi_0(\mathbf{r})$ is real, which is always possible to achieve for a bound state, and normalized by

$$\int \psi_0^2(\mathbf{r})\,d\mathbf{r} = 1. \tag{26}$$

Within the standard perturbation theory [17], the solution to Eq. (1) for $F > 0$ originating from this bound state is given by

$$\mathcal{E} = E_0 - \mu_z F - \tfrac{1}{2}\alpha_{zz}F^2 + O(F^3), \tag{27a}$$

$$\psi(\mathbf{r}) = \psi_0(\mathbf{r}) + \psi_1(\mathbf{r})F + O(F^2). \tag{27b}$$

Here μ_z and α_{zz} are the components of the electronic dipole moment vector μ_i and the static dipole polarizability tensor

α_{ij}, $i,j = x,y,z$, in the unperturbed state $\psi_0(\mathbf{r})$, respectively, and

$$\int \psi_1(\mathbf{r})\psi_0(\mathbf{r})\,d\mathbf{r} = 0, \tag{28}$$

so that the function (27b) satisfies the normalization condition (19) with an error of order $O(F^2)$. The series (27) are known to have two important shortcomings. First, all terms in these series, up to any finite order in F, are real. Thus Eq. (27a) defines only the real part of the complex SS eigenvalue (18); the ionization rate Γ is exponentially small in F and cannot be accounted for by a power series. Second, Eq. (27b) holds only in the region $\eta \ll 2|E_0|/F$, where the field term in Eq. (15) can be treated perturbatively. The right-hand side of Eq. (27b) exponentially decays in the asymptotic region, where the outgoing wave (17) is formed, so this expansion does not allow one to find the coefficients f_ν, which are also exponentially small in F. To calculate f_ν and then Γ one has to connect Eq. (27b) with Eq. (17) by solving Eq. (15). In the weak-field limit (24) this can be done by asymptotic methods [27,28].

In the following, we assume that all quantities appearing in Eqs. (27) are known. They can, for example, be obtained by calculations in a finite volume, where various efficient numerical techniques can be used. Our goal is to express observables related to tunneling ionization in terms of these quantities.

B. Parabolic channels

The parabolic channels are defined by Eqs. (8) and (9), where one should substitute $\mathcal{E}$ given by Eq. (27a) for E into Eq. (9a). The solution to this eigenvalue problem can be found using perturbation theory,

$$\beta_\nu = \beta_\nu^{(0)} + \beta_\nu^{(1)}F + O(F^2), \tag{29a}$$

$$\phi_\nu(\xi) = \phi_\nu^{(0)}(\xi) + \phi_\nu^{(1)}(\xi)F + O(F^2). \tag{29b}$$

The zeroth-order terms in these expansions were obtained in Ref. [16],

$$\beta_\nu^{(0)} = Z - \varkappa\left(n_\xi + \frac{|m|+1}{2}\right), \tag{30a}$$

$$\phi_\nu^{(0)}(\xi) = \varkappa^{1/2}(\varkappa\xi)^{|m|/2}e^{-\varkappa\xi/2}\sqrt{\frac{n_\xi!}{(n_\xi+|m|)!}}\,L_{n_\xi}^{(|m|)}(\varkappa\xi), \tag{30b}$$

where $L_n^{(\alpha)}(x)$ are the generalized Laguerre polynomials [26]. Here we obtain the first-order terms,

$$\beta_\nu^{(1)} = -\frac{\mu_z}{2\varkappa}(2n_\xi + |m| + 1) - \frac{1}{4\varkappa^2}\left[6n_\xi(n_\xi+|m|+1) + m^2 + 3|m| + 2\right], \tag{31a}$$

$$\phi_\nu^{(1)}(\xi) = \frac{1}{8\varkappa^3}\{c_{n_\xi-2}c_{n_\xi-1}\phi_{n_\xi-2,m}^{(0)}(\xi) - 4c_{n_\xi-1} \times [\varkappa\mu_z + (2n_\xi+|m|)]\phi_{n_\xi-1,m}^{(0)}(\xi) + 4c_{n_\xi}[\varkappa\mu_z + (2n_\xi+|m|+2)]\phi_{n_\xi+1,m}^{(0)}(\xi) - c_{n_\xi}c_{n_\xi+1}\phi_{n_\xi+2,m}^{(0)}(\xi)\}, \tag{31b}$$

where

$$c_{n_\xi} = \sqrt{(n_\xi+1)(n_\xi+|m|+1)} \tag{32}$$

and it is implied that the functions $\phi_{n_\xi m}^{(0)}(\xi)$ with negative n_ξ in Eq. (31b) are equal to zero. Substituting Eq. (29b) into Eq. (8a), we obtain the corresponding expansion for the parabolic channel functions,

$$\Phi_\nu(\xi,\varphi) = \Phi_\nu^{(0)}(\xi,\varphi) + \Phi_\nu^{(1)}(\xi,\varphi)F + O(F^2). \tag{33}$$

C. Asymptotic coefficients

Here we find the coefficient f_ν in Eq. (17). To this end, we need to connect Eq. (27b) with Eq. (17) by constructing the asymptotic solution of the uncoupled equations (15). This is done in Appendix A; here we invoke the results obtained there. The correspondence between Eq. (A1) treated in Appendix A and Eq. (15) is established by identifying the coefficients E, β, and γ in Eq. (A1) with $\mathcal{E}$, β_ν, and γ_m given by Eqs. (27a), (29a), and (16), respectively. Substituting Eqs. (27a) and (29a) into the equations of Appendix A, one should perform an additional expansion in F. In this way from Eq. (A13) we obtain the solution to Eq. (15) in the region $1 \ll \eta \ll F^{-1/2}$ [here we assume that $\eta > \eta_c$, which is always possible to achieve since $\eta_c = O(F^0)$]:

$$f_\nu(\eta) = g_\nu\eta^{\beta_\nu^{(0)}/\varkappa}e^{-\varkappa\eta/2}\{1 + O(\eta^{-1}) + [C_2\eta^2 + C_1\eta + C_l\ln\eta + C_0 + a_\nu + O(\eta^{-1}\ln\eta)]F + O(F^2)\}, \tag{34}$$

where

$$C_2 = (8\varkappa)^{-1}, \tag{35a}$$

$$C_1 = -\frac{\mu_z}{2\varkappa} + \frac{2-\gamma_m}{8\varkappa^2} + \frac{5\beta_\nu^{(0)}}{8\varkappa^3} - \frac{\beta_\nu^{(0)2}}{8\varkappa^4}, \tag{35b}$$

$$C_l = \frac{\beta_\nu^{(1)}}{\varkappa} + \frac{\gamma_m - 2\mu_z\beta_\nu^{(0)}}{2\varkappa^3} + \frac{3\beta_\nu^{(0)2}}{2\varkappa^5}, \tag{35c}$$

$$C_0 = \frac{\mu_z}{2\varkappa^2}\left(\gamma_m - \frac{\beta_\nu^{(0)}}{\varkappa} + \frac{\beta_\nu^{(0)2}}{\varkappa^2}\right). \tag{35d}$$

Expansion (34) contains two unknown field-independent coefficients, g_ν and a_ν, which can be found by matching it with Eq. (27b). Indeed, from Eq. (11) we have

$$\eta^{-1/2}f_\nu(\eta) = \langle\Phi_\nu|\psi(\mathbf{r})\rangle = \langle\Phi_\nu^{(0)}|\psi_0(\mathbf{r})\rangle + \left[\langle\Phi_\nu^{(1)}|\psi_0(\mathbf{r})\rangle + \langle\Phi_\nu^{(0)}|\psi_1(\mathbf{r})\rangle\right]F + O(F^2). \tag{36}$$

By comparing this with Eq. (34), we find

$$g_\nu = \eta^{1/2-\beta_\nu^{(0)}/\varkappa}e^{\varkappa\eta/2}\langle\Phi_\nu^{(0)}|\psi_0(\mathbf{r})\rangle_{\eta\to\infty} \tag{37}$$

and

$$a_\nu = g_\nu^{-1}\eta^{1/2-\beta_\nu^{(0)}/\varkappa}e^{\varkappa\eta/2}\left[\langle\Phi_\nu^{(1)}|\psi_0(\mathbf{r})\rangle + \langle\Phi_\nu^{(0)}|\psi_1(\mathbf{r})\rangle\right]_{\eta\to\infty} - (C_2\eta^2 + C_1\eta + C_l\ln\eta + C_0). \tag{38}$$

Having thus defined g_ν and a_ν, we obtain from Eq. (A25)

$$f_\nu = \frac{\varkappa^{1/2} g_\nu}{2^{1/2}} \left(\frac{4\varkappa^2}{F}\right)^{\beta_\nu^{(0)}/\varkappa} \exp\left[\frac{i\pi}{4} + \frac{i\pi\beta_\nu^{(0)}}{\varkappa} - \varkappa\mu_z - \frac{\varkappa^3}{3F}\right] \times \left[1 + \frac{1}{2} A_\nu F \ln\frac{F}{4\varkappa^2} + \frac{1}{2}(B_\nu + 2i \ \mathrm{Im}\ a_\nu - i\pi A_\nu)F + O(F^2)\right], \tag{39}$$

where

$$A_\nu = -\frac{2\beta_\nu^{(1)}}{\varkappa} - \frac{\gamma_m - 2\mu_z\beta_\nu^{(0)}}{\varkappa^3} - \frac{3\beta_\nu^{(0)2}}{\varkappa^5}, \tag{40a}$$

$$B_\nu = -\varkappa\alpha_{zz} - \frac{\mu_z^2}{\varkappa} + \frac{\mu_z}{\varkappa^2} + \frac{4\mu_z\beta_\nu^{(0)}}{\varkappa^3} - \frac{10 + 18\gamma_m + 3\gamma_m^2}{24\varkappa^3} - \frac{(9 - 6\gamma_m)\beta_\nu^{(0)}}{4\varkappa^4} - \frac{(49 + 2\gamma_m)\beta_\nu^{(0)2}}{8\varkappa^5} + \frac{3\beta_\nu^{(0)3}}{2\varkappa^6} - \frac{\beta_\nu^{(0)4}}{8\varkappa^7} + 2\ \mathrm{Re}\ a_\nu. \tag{40b}$$

Note that g_ν and a_ν are generally complex and for real $\psi_0(\mathbf{r})$ and $\psi_1(\mathbf{r})$ they satisfy

$$g_{n_\xi,-m} = g^*_{n_\xi m}, \quad a_{n_\xi,-m} = a^*_{n_\xi m}, \tag{41}$$

while A_ν and B_ν are real. Equation (39) generalizes Eq. (57) from Ref. [16].

D. Ionization rate

In the weak-field limit (24), the ionization rate Γ is equal to the total flux of ionized electrons and therefore can be expressed in terms of the coefficients f_ν in Eq. (17). This expression was already given in Ref. [16], but it is worthwhile to reiterate its derivation on the basis of the present diabatic expansion (11). From Eqs. (1) and (18) we have

$$\Gamma|\psi(\mathbf{r})|^2 = \nabla\mathbf{j}(\mathbf{r}), \tag{42}$$

where

$$\mathbf{j}(\mathbf{r}) = \frac{-i}{2}[\psi^*(\mathbf{r})\nabla\psi(\mathbf{r}) - \psi(\mathbf{r})\nabla\psi^*(\mathbf{r})]. \tag{43}$$

The imaginary part of $\psi(\mathbf{r})$ is exponentially small in F and can be neglected on the left-hand side of Eq. (42) (but not on its right-hand side). Then, integrating both sides of this equation and using the normalization condition (19), we obtain

$$\Gamma = \int_{S_\eta} \mathbf{e}_\eta \cdot \mathbf{j}(\mathbf{r})\, dS_\eta \Big|_{\eta\to\infty}, \tag{44}$$

where S_η is a surface of constant η, $\mathbf{e}_\eta$ is the unit normal vector to S_η pointing toward $\eta \to \infty$, and dS_η is the area element of S_η. We have

$$dS_\eta = \sqrt{\frac{r\eta}{2}}\, d\xi\, d\varphi, \quad \mathbf{e}_\eta \cdot \nabla = \sqrt{\frac{2\eta}{r}}\,\frac{\partial}{\partial\eta}, \tag{45}$$

and hence

$$\Gamma = \frac{-i\eta}{2}\int_0^\infty d\xi \int_0^{2\pi} d\varphi \left[\psi^*(\mathbf{r})\frac{\partial}{\partial\eta}\psi(\mathbf{r}) - \psi(\mathbf{r})\frac{\partial}{\partial\eta}\psi^*(\mathbf{r})\right]_{\eta\to\infty}. \tag{46}$$

Substituting here Eq. (11), using Eqs. (10) and (17), and noting that the imaginary part of E is exponentially small in F and can be neglected in Eqs. (9a) and (17), we obtain [16]

$$\Gamma = \sum_\nu \Gamma_\nu + O(\Gamma^2), \quad \Gamma_\nu = |f_\nu|^2. \tag{47}$$

Here Γ_ν is the partial rate corresponding to ionization into parabolic channel ν and the error term $O(\Gamma^2)$ arises from the exponentially small contributions neglected in the derivation. We note that in the same approximation from Eqs. (22) and (23) we have [16]

$$\Gamma = \int P(\mathbf{k}_\perp)\frac{d\mathbf{k}_\perp}{(2\pi)^2} + O(\Gamma^2), \tag{48}$$

which is consistent with the physical meaning of Γ and $P(\mathbf{k}_\perp)$. Substituting Eq. (39) into Eq. (47), we find

$$\Gamma_\nu = |G_\nu|^2 W_\nu(F)\left[1 + A_\nu F \ln\frac{F}{4\varkappa^2} + B_\nu F + O(F^2)\right], \tag{49}$$

where G_ν and $W_\nu(F)$ are the standard *structure* and *field* factors [22,23],

$$G_\nu = e^{-\varkappa\mu_z} g_\nu, \tag{50}$$

$$W_\nu(F) = \frac{\varkappa}{2}\left(\frac{4\varkappa^2}{F}\right)^{2Z/\varkappa - 2n_\xi - |m| - 1} \exp\left(-\frac{2\varkappa^3}{3F}\right), \tag{51}$$

and the *correction* coefficients A_ν and B_ν are defined by Eqs. (40). Equation (49) generalizes Eq. (60) from Ref. [16].

Now, when the asymptotic coefficient f_ν is converted into the partial ionization rate Γ_ν, which is a more transparent quantity, it is worthwhile to list the physical effects resulting in the appearance of the correction terms in Eqs. (39) and (49). The first is the first-order correction to the eigenvalue (29a) of the Hamiltonian (6) generating the parabolic channels. This correction is related to a modification of the Runge-Lenz vector of the active electron when it is outside the core region by the external electric field. It contributes to A_ν in Eq. (40a). The second is the second-order Stark shift of the energy (27a) of the state defined by the polarizability α_{zz}. The third is the distortion of the unperturbed bound-state orbital represented by the second term in Eq. (27b) and characterized by the coefficient a_ν defined by Eq. (38). The latter two corrections contribute to B_ν in Eq. (40b). The fourth is the dipole term in Eq. (2), which enters the definition of γ_m in Eq. (16). Finally, the fifth is a correction to the asymptotic solution of the uncoupled equations (15). The latter two corrections contribute to both A_ν and B_ν. All these effects must be taken into account to obtain the exact values of the correction coefficients A_ν and B_ν.

The partial ionization rates (49) for the different channels have the same exponential factor but different powers of F in Eq. (51). The power of F grows by 2 and 1 as n_ξ or $|m|$ are increased by unity, respectively. Therefore in the leading-order approximation one should retain in the total ionization rate (47) only the contribution from the *dominant* channel, the one with the minimum values of n_ξ and $|m|$ for which $g_\nu \neq 0$ [16]. However, including the first-order correction terms for the

dominant channel in Eq. (49), one should also retain in Eq. (47) the leading-order approximation for contributions from the *next-to-the-dominant* channels, the ones with the same n_ξ and $|m|$ increased by unity, which have the same power of F. The dominant channel is determined by the symmetry of the potential. Three symmetry cases should be distinguished [16]. Below we give final formulas for the total ionization rate in these cases.

(a) *Potentials without any symmetry*. This corresponds to arbitrary molecules arbitrarily oriented with respect to the field. In this case, all the coefficients g_ν are generally nonzero, the dominant channel is $\nu = (0,0)$, and there are two next-to-the-dominant channels $(0, \pm 1)$. From Eqs. (47) and (49) we obtain

$$\Gamma \approx W_{00}(F)\left[|G_{00}|^2\left(1 + A_{00}F\,\ln\frac{F}{4\varkappa^2} + B_{00}F\right) + \frac{F}{2\varkappa^2}\,|G_{01}|^2\right]. \tag{52}$$

(b) *Axially symmetric potentials*. This corresponds to atoms and linear molecules aligned along the field. In this case, $V(\mathbf{r}) = V(\xi,\eta)$ and Eq. (1) has solutions of the form $\psi(\mathbf{r}) = \psi(\xi,\eta)e^{im\varphi}$, for which m is an exact quantum number [14]. For $m \neq 0$, the solutions $\propto e^{\pm im\varphi}$ are degenerate, so one can switch to another pair of solutions proportional to $\cos m\varphi$ and $\sin m\varphi$. According to our convention, $\psi_0(\mathbf{r})$ is real, which corresponds to the latter representation. Then the sums in Eqs. (11) and (47) contain only channels with $\nu = (n_\xi, \pm|m|)$. There is one dominant channel $(0,0)$, for $m = 0$, and two dominant channels $(0, \pm|m|)$, for $m \neq 0$, but there are no next-to-the-dominant channels. It can be seen that all the coefficients in Eq. (49) in this case depend only on the absolute value of m. Thus for states with a given m we obtain

$$\Gamma \approx (2 - \delta_{m0})|G_{0m}|^2 W_{0m}(F)\left(1 + A_{0m}F\,\ln\frac{F}{4\varkappa^2} + B_{0m}F\right). \tag{53}$$

For $m = 0$ this formula coincides with Eq. (52), taking into account that in the present case $G_{01} = 0$.

(c) *The Coulomb potential*. For a purely Coulomb potential, Eq. (1) allows separation of variables in parabolic coordinates [17], so both quantum numbers n_ξ and m identifying the parabolic channels are exact. In this case, it is convenient to switch to a more conventional representation in which the solutions to Eq. (1) depend on φ as $e^{im\varphi}$. Let us consider the hydrogen atom in a state with parabolic quantum numbers (n_ξ, n_η, m) ($n_\xi \equiv n_1$ and $n_\eta \equiv n_2$ in the notation of Ref. [17]). Then the sums in Eqs. (11) and (47) contain only one channel with $\nu = (n_\xi, m)$; this is the dominant channel and there are no next-to-the-dominant channels. For hydrogen $Z = 1$, $\mathbf{D} = \mathbf{0}$, and $\alpha_{ij} = \alpha\delta_{ij}$. The values of E_0, μ_z, and α are well known [17]. Substituting all these into Eq. (40a), we find $A_\nu = 0$. Thus

$$\Gamma \approx |G_\nu|^2 W_\nu(F)(1 + B_\nu F). \tag{54}$$

We have

$$\psi_0(\mathbf{r}) = \frac{\sqrt{2}}{n}\,\phi^{(0)}_{n_\eta m}(\eta)\Phi^{(0)}_\nu(\xi,\varphi), \tag{55a}$$

$$\psi_1(\mathbf{r}) = \frac{\sqrt{2}}{n}\left[\phi^{(0)}_{n_\eta m}(\eta)\Phi^{(1)}_\nu(\xi,\varphi) - \tilde\phi^{(1)}_{n_\eta m}(\eta)\Phi^{(0)}_\nu(\xi,\varphi)\right] + \frac{3}{4}\,n^3(n_\xi - n_\eta)\psi_0(\mathbf{r}), \tag{55b}$$

where $n = n_\xi + n_\eta + |m| + 1$ is the principle quantum number and $\tilde\phi^{(1)}_{nm}(x)$ coincides with $\phi^{(1)}_{nm}(x)$ defined by Eq. (31b) with the sign of μ_z changed to the opposite. Note that the functions (55) satisfy Eqs. (26) and (28), where one of the factors in the integrand is to be replaced by its complex conjugate, because of the factor $e^{im\varphi}$. Substituting Eq. (55a) into Eq. (37), we reproduce Eq. (67) from Ref. [16],

$$g_\nu = \frac{(-1)^{n_\eta}\sqrt{2}}{n^{n_\eta + |m|/2 + 3/2}\sqrt{n_\eta!(n_\eta + |m|)!}}. \tag{56}$$

Substituting Eq. (55b) into Eq. (38), we find

$$a_\nu = \frac{n^3}{16}\left[n_\eta^4 + (2|m| - 10)n_\eta^3 + (m^2 - 15|m| - 11)n_\eta^2 - (5m^2 + 24n_\xi + 23|m| + 36)n_\eta - 6(2n_\xi + |m| + 3)|m| - 12\right]. \tag{57}$$

With these values of g_ν and a_ν, Eq. (54) is *in full agreement* with the result obtained by a different method in Ref. [24]. We note that the method of Ref. [24] is applicable only to the Coulomb potential, when the variables in Eq. (1) can be separated, while the present approach applies to arbitrary potentials. This agreement provides an independent confirmation of the consistency of the present approach and results.

E. Transverse momentum distribution

The weak-field asymptotic expansion for the TMD (23) can be obtained by substituting Eqs. (33) and (39) into Eq. (22). In calculating the sum in Eq. (22), one should again retain all channels whose contributions have the same power of F as the correction terms in Eq. (39) for the dominant channel. Here we give the final formula only for the case when the dominant channel is $\nu = (0,0)$. In this case, one should retain in Eq. (22) also the contributions from channels $(0, \pm 1)$, $(0, \pm 2)$, and $(1,0)$. The TMD is thus given by

$$P(\mathbf{k}_\perp) \approx \frac{4\pi\varkappa}{F}\,W_{00}(F)e^{-s}\left[G_{00}^2\left(1 + A_{00}F\,\ln\frac{F}{4\varkappa^2} + \left\{B_{00} + \frac{1}{4\varkappa^3}[6 + 4\varkappa\mu_z - 4(\varkappa\mu_z + 1)s - s^2]\right\}F\right) - \{(1 - s)G_{00}G_{10} - 2s[\mathrm{Re}(G_{01}e^{i\varphi_k})]^2 + \sqrt{2}sG_{00}\,\mathrm{Re}(G_{02}e^{2i\varphi_k})\}\frac{F}{2\varkappa^2}\right], \tag{58}$$

where

$$s = \frac{\varkappa k_\perp^2}{F}, \tag{59}$$

and we have explicitly used that $G_{n_\xi,-m} = G^*_{n_\xi m}$, which follows from the first of Eqs. (41). Equation (58) generalizes Eq. (64) from Ref. [16]. It applies to potentials without any symmetry, but also to states with $m = 0$ in axially symmetric potentials, when $G_{01} = G_{02} = 0$, and to the ground state of

hydrogen, when $G_{01} = G_{02} = G_{10} = 0$. In the latter case it reduces to

$$P(\mathbf{k}_\perp) \approx \frac{16\pi}{F^2} \exp\left(-\frac{2}{3F} - s\right)\left[1 - \left(\frac{89}{12} + s + \frac{s^2}{4}\right)F\right]. \tag{60}$$

The exponential factor e^{-s} in Eqs. (58) and (60) results in a well-known Gaussian shape of the TMD in the weak-field limit, $P(\mathbf{k}_\perp) \propto \exp(-\varkappa k_\perp^2/F)$. This shape was first obtained within the static limit of the Keldysh theory [29,30] and later was reproduced by different methods by other authors [16,31, 32]. The s-dependent part of the correction terms in Eqs. (58) and (60) accounts for a departure from the Gaussian shape at stronger fields, while the s-independent part accounts for a change of the magnitude of the TMD corresponding to a departure of Γ from the leading-order term in Eq. (52), in accordance with Eq. (48).

F. Region of applicability

Mathematically, the asymptotic solution of the SS eigenvalue problem developed in this section applies in the limit (24). Physically, however, it is desirable to indicate the upper boundary of the interval of F where the expansions obtained hold. The region of applicability of the WFAT can be specified by the condition [16]

$$F \ll F_c, \tag{61}$$

where the critical field F_c is a boundary between the tunneling and over-the-barrier ionization regimes. The value of F_c can be estimated as the field for which the two turning points of Eq. (15) for the dominant channel coalesce. Substituting for E and β_ν the leading-order terms from Eqs. (27a) and (29a), we obtain

$$F_c \approx \frac{\varkappa^4}{8|2Z - \varkappa(2n_\xi + |m| + 1)|}, \tag{62}$$

where n_ξ and m correspond to the dominant channel. The condition (61) ensures that the first-order correction terms in Eqs. (39) and (49) are much smaller than unity. In practice, we shall see that these corrections remain meaningful, that is, improve the leading-order results, up to $F \sim F_c$.

IV. ILLUSTRATIVE CALCULATIONS

The derivation in Sec. III of the first-order correction terms in the asymptotic expansions of the ionization rate and TMD within the WFAT is general and covers atomic (spherically symmetric potentials) as well as molecular (arbitrary potentials without any symmetry) cases. In this first illustration of the results obtained we restrict our treatment to the atomic case when accurate calculations of the coefficients required to implement the theory can be performed relatively easily. We consider hydrogen and four noble-gas atoms. In all cases the asymptotic charge seen by the outgoing electron is $Z = 1$, the dipole of the atomic ion is $\mathbf{D} = \mathbf{0}$ [see Eq. (2)], the polarizability tensor reduces to a scalar $\alpha_{ij} = \alpha\delta_{ij}$, and the TMD (23) depends only on the absolute value of the transverse momentum and is denoted by $P(k_\perp)$. We compare the ionization rate and TMD predicted by the WFAT with the results of accurate numerical calculations. For brevity, the leading-order WFAT results and those including the first-order corrections are denoted by WFAT(0) and WFAT(1), respectively, and the accurate numerical results are referred to as "exact."

A. Hydrogen

We first consider hydrogen for which earlier theories including higher-order corrections in the field strength for the ionization rate are available [24,25]. In this case, all the coefficients needed to implement the present theory are known analytically [see Eqs. (56) and (57)]. The exact results are obtained by the procedure outlined in Appendix B.

In Fig. 1, we show the ionization rate for the ground state divided by the field factor (51) with $\nu = (0,0)$. In this representation, rapid variation of Γ by many orders of magnitude as $F \to 0$ is eliminated, which facilitates comparison of the different results. As detailed in the caption, labels WFAT(n) refer to the results obtained by including terms up to order F^n in the asymptotic expansion of Γ. The WFAT(0) and WFAT(1) results are obtained from Eq. (54) omitting the linear in F term and including this term with $B_{00} = -107/12$, respectively. The WFAT(2) and WFAT(10) results are obtained by adopting the coefficients of higher powers of F given in Ref. [25]. The good agreement between the WFAT(1) and the exact results at $F \lesssim 0.02$ confirms the second term in Eq. (54). We note that although the value of B_{00} has been known for a long time [24,25], its unambiguous confirmation by accurate calculations was hindered by extremely small values of Γ at such small F where Eq. (54) holds with sufficient accuracy. To overcome this difficulty, which is needed for validating the asymptotic results, we have developed a multiple-precision procedure discussed in Appendix B. The departure of the WFAT(1) from the exact results at larger fields is caused by the presence of higher-order terms in the asymptotic expansion. Figure 1 illustrates quantitatively how much such higher-order

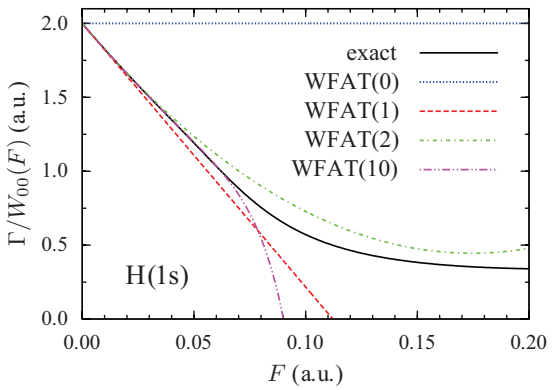

FIG. 1. (Color online) Ratio of the ionization rate to the field factor (51) as a function of field for hydrogen in the ground state. Solid (black) line: exact results. Dotted (blue) line, WFAT(0): the leading-order WFAT results obtained by omitting the linear in F correction term in Eq. (54). Dashed (red) line, WFAT(1): the WFAT results including the first-order correction in F, Eq. (54). Dotted-dashed (green) line, WFAT(2), and dashed-double-dotted (magenta) line, WFAT(10): results from Ref. [25] including terms up to order F^2 and F^{10}, respectively, in the asymptotic expansion for Γ.

corrections improve the prediction of the WFAT. For any given $F < F_c$, the inclusion of terms up to certain maximum order improves the results, but incorporating further terms makes the results only worse. The smaller F, the larger this maximum order, and the higher accuracy can be achieved. Thus, for example, at $F = 0.05$ the WFAT(10) is closer to the exact results than WFAT(1), but at $F = 0.1$ the opposite is true. Such a behavior reflects a well-known property of divergent asymptotic series; a good illustration of this point on the example of the perturbation-theory series (27a) for the real part of the energy of the ground state can be found in Ref. [33]. In contrast to the WFAT(0), which yields at least a positive value of Γ for any field, the WFAT(1) cannot be extended beyond $F_c = -1/B_{00} \approx 0.112$, where the right-hand side of Eq. (54) turns zero, which again reflects the asymptotic nature of the expansion. This value of F_c is slightly lower than $F_c = 0.125$ obtained from Eq. (62) and gives a better estimate of the boundary for over-the-barrier ionization. The main conclusion to be drawn from Fig. 1 is that the first-order correction included in WFAT(1) significantly improves the prediction for Γ as compared to WFAT(0), extending the region of applicability of the theory up to $F \sim F_c$, while the higher-order terms can be safely neglected in this region within a tolerable error. For example, the WFAT(1) remains valid within an error of 20% up to $F = 0.076$, while the WFAT(0) is beyond this error already at $F = 0.020$. We will see that this conclusion applies also to other atoms.

The excited states of hydrogen are also of interest to investigate with the present theory. In this case, for states with $n_\xi \neq n_\eta$, there exists a permanent dipole moment $\mu_z = -3n(n_\xi - n_\eta)/2$ which modifies the structure factor (50) and also contributes to the coefficient B_ν in Eq. (54). In Fig. 2, we compare the exact results with the WFAT(0) and WFAT(1), again focusing on the ratio of the rate and the field factor (51) which enables one to compare the results quantitatively. We consider the three states with $n = 2$ and $(n_\xi, n_\eta, m) = (1,0,0)$, $(0,1,0)$, and $(0,0,1)$, which are degenerate in the absence of the field. The first two of these states have nonzero dipoles of the same value but different sign. Due to the presence of this dipole in the exponent in Eq. (50), and the corresponding polarization of the electron density, there is a large difference in the magnitude of the ionization rates for these states. The third state with $m = 1$ does not have a dipole and its rate takes values between the two other states. Figure 2 shows that in all cases a significant improvement on the step from WFAT(0) to WFAT(1) in agreement with the exact results is achieved. The convergence of the WFAT(1) with the exact results as F decreases confirms the linear in F term in Eq. (54), including the case of states with a permanent dipole. This illustrates that our theory correctly treats polar systems, a typical situation for molecules.

We now turn to a discussion of the accuracy of the WFAT in predicting the TMD. Together with the complex SS eigenvalue (18), the TMD (23) presents an essential characteristic required for implementing the adiabatic theory [13], so it is instructive to see in which region of the field strengths the WFAT can be used instead of much more time-consuming exact calculations. We consider only the ground state. The results for two representative values of F are shown in Fig. 3. The WFAT(0) and WFAT(1) results are obtained from Eq. (60) omitting

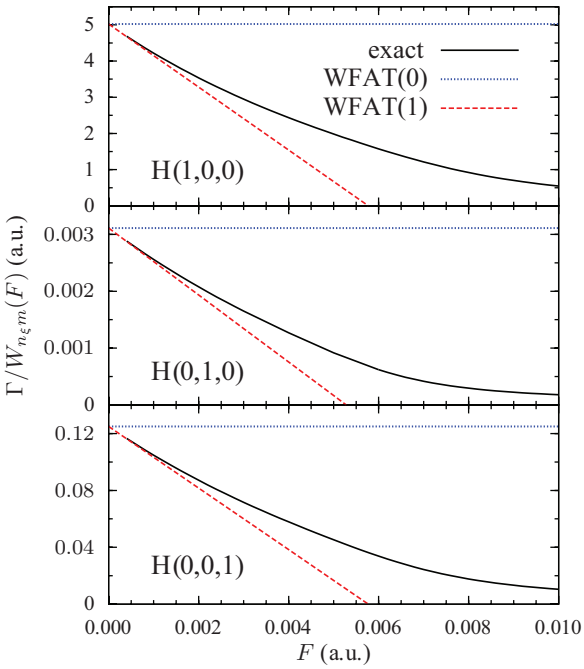

FIG. 2. (Color online) Ratio of the ionization rate to the field factor (51) as a function of field for hydrogen in states with parabolic quantum numbers (n_ξ, n_η, m) indicated in the figure. Solid (black) lines: exact results. Dotted (blue) lines, WFAT(0): the leading-order WFAT results. Dashed (red) lines, WFAT(1): the WFAT results including the first-order correction in F, Eq. (54).

and including the linear in F correction term, respectively. The exact results are calculated using the general method developed in Ref. [14]. Figure 3 shows that the WFAT(1) prediction is in much better agreement with the exact results than the WFAT(0). This is not a surprise, because the field values considered belong to the interval where Eq. (54) works well. The improvement of WFAT(1) over WFAT(0) is mainly

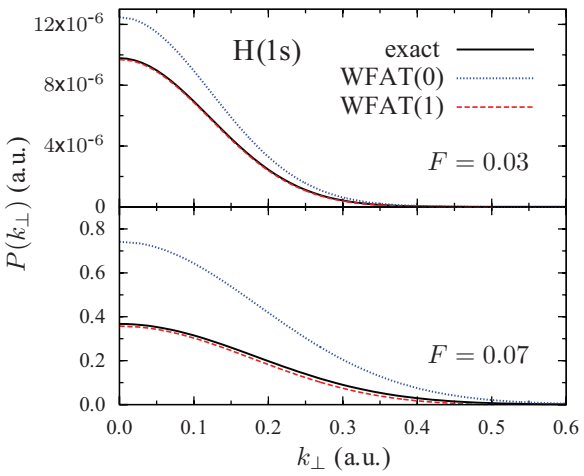

FIG. 3. (Color online) Transverse momentum distributions for hydrogen in the ground state at two representative values of the field F. Solid (black) lines: exact results. Dotted (blue) lines, WFAT(0): the leading-order WFAT results obtained by omitting the linear in F correction term in Eq. (60). Dashed (red) line, WFAT(1): the WFAT results including the first-order correction in F, Eq. (60).

TABLE I. Characteristics of noble-gas atoms. The number of electrons N and the parameters u and v define the effective charge (64) in the one-electron model potential (63). E_0 is the unperturbed bound-state energy of the active electron and α is its polarizability. The asymptotic coefficients g_{00}, g_{10}, and a_{00} are defined by Eqs. (37) and (38). The correction coefficients A_{00} and B_{00} are defined by Eqs. (40). All values are given in atomic units.

Atom	N	u	v	E_0	α	g_{00}	g_{10}	a_{00}	A_{00}	B_{00}
Ne($2p$)	10	1.704	2.810	−0.793	0.152	2.1	3.7	−0.8	0.246	− 2.6
Ar($3p$)	18	0.933	3.600	−0.579	1.323	2.7	5.3	−2.1	0.158	− 7.7
Kr($4p$)	36	1.340	4.311	−0.515	2.099	2.3	4.6	−2.8	0.042	−10.5
Xe($5p$)	54	1.048	5.197	−0.446	3.079	2.5	5.2	−4.8	−0.222	−16.4

attributed to the s-independent part of the correction term in Eq. (60) (see the discussion after that equation). The investigation of a more subtle effect of the departure of the shape of the TMD from the Gaussian, which is accounted for by the s-dependent part of the correction term, is postponed to the end of the next section.

B. Noble-gas atoms

We proceed with calculations for the noble-gas atoms Ne, Ar, Kr, and Xe. The active electron in these atoms is described by the $2p$, $3p$, $4p$, and $5p$ states, respectively, with azimuthal quantum number $m = 0$ in all cases, in a local spherically symmetric potential of the form [34,35]

$$V(r) = -\frac{Z_{\rm eff}(r)}{r}, \tag{63}$$

where the effective charge $Z_{\rm eff}(r)$ monotonically decreases from the bare nuclear charge equal to the number of electrons N, at $r = 0$, to 1, at $r \to \infty$, and is given by

$$Z_{\rm eff}(r) = N - (N-1)\{1 - [(v/u)(e^{ur} - 1) + 1]^{-1}\}. \tag{64}$$

Equations (63) and (64) comply with Eq. (2). The recommended values of the parameters u and v are given in Table I.

All the atomic characteristics needed to implement the WFAT are also given in Table I. For all atoms, the dominant channel is $\nu = (0,0)$ and the dipole moment is $\mu_z = 0$. The unperturbed bound-state energy E_0 and wave function $\psi_0(\mathbf{r})$ are obtained using the Laguerre discrete variable representation [36] in parabolic coordinates. The same procedure yields a complete discrete set of the eigenstates of the unperturbed Hamiltonian in the functional space spanned by the Laguerre basis. The polarizability α and the first-order correction $\psi_1(\mathbf{r})$ to the wave function are then calculated by implementing standard spectral expansions of perturbation theory [17]; a

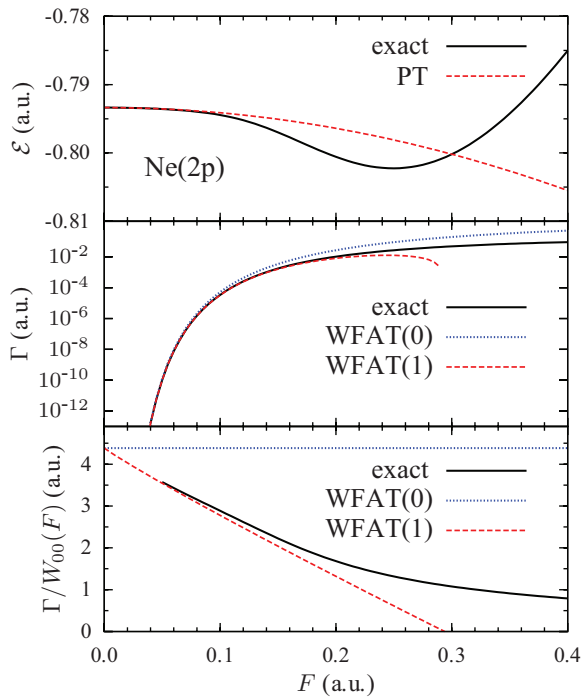

FIG. 4. (Color online) Real part of the energy (top panel), ionization rate (middle panel), and its ratio to the structure factor (51) (bottom panel) as functions of field for Ne($2p$). Solid lines: exact results. Dashed (red) line in the top panel: perturbation theory, Eq. (27a). Dotted (blue) lines in the lower two panels, WFAT(0): the leading-order WFAT results obtained by omitting the first-order correction terms in Eq. (53). Dashed (red) lines in the lower two panels, WFAT(1): the WFAT results including the first-order correction, Eq. (53).

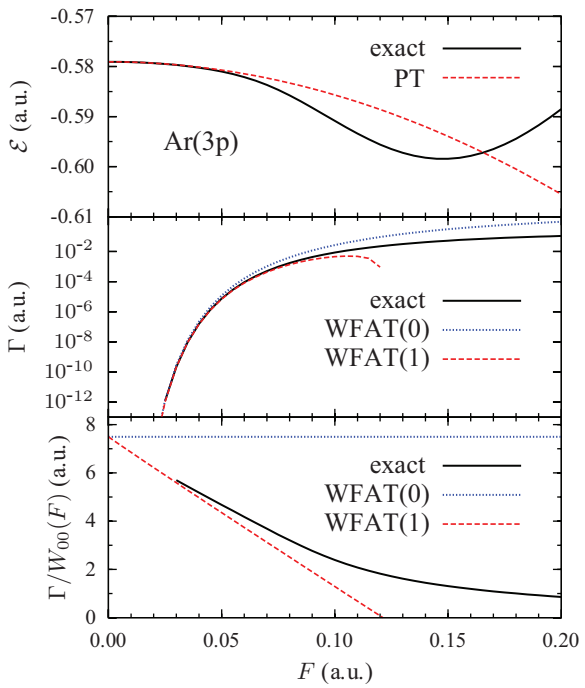

FIG. 5. (Color online) Same as in Fig. 4, but for Ar($3p$).

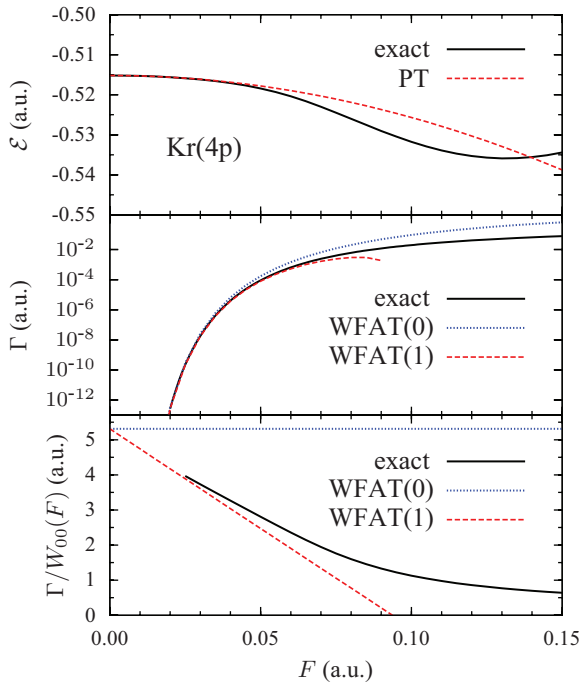

FIG. 6. (Color online) Same as in Fig. 4, but for Kr($4p$).

similar procedure using the Legendre basis in a finite box in spherical coordinates was described in Ref. [15]. The coefficients g_{00}, g_{10}, and a_{00} are obtained from Eqs. (37) and (38) by a fitting procedure outlined in Ref. [23] applied at sufficiently large values of η. From Eq. (50) in the present case we have $G_{00} = g_{00}$ and $G_{10} = g_{10}$. The correction coefficients A_{00} and B_{00} are found from Eqs. (40). Note that A_{00} as a function of $\varkappa$ turns zero for $\varkappa = 1$, which corresponds to $E_0 = -0.5$. This explains the small value of this coefficient

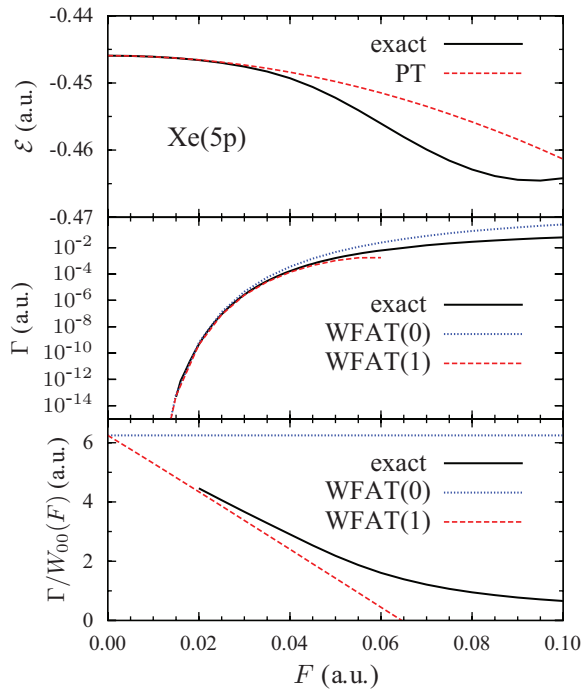

FIG. 7. (Color online) Same as in Fig. 4, but for Xe($5p$).

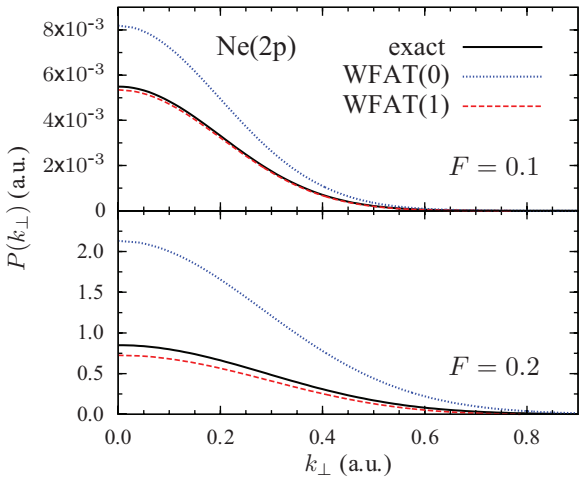

FIG. 8. (Color online) Transverse momentum distributions for Ne($2p$) at two representative values of the field F. Solid (black) lines: exact results. Dotted (blue) lines, WFAT(0): the leading-order WFAT results obtained by omitting the first-order correction terms in Eq. (58). Dashed (red) lines, WFAT(1): the WFAT results including the first-order correction, Eq. (58).

for Kr($4p$) and its different sign for Xe($5p$). The WFAT results for the ionization rate and TMD are obtained from Eq. (53) with $m = 0$ and Eq. (58) with $G_{01} = G_{02} = 0$, respectively. For completeness, we also present exact results for the real part of the SS eigenvalue (18) and compare them with the perturbation-theory expansion (27a). The exact results in all cases are calculated using the method of Ref. [14].

Figures 4–7 show the energy $\mathcal{E}$, ionization rate Γ, and its ratio to the field factor (51) as functions of F for the four atoms. The perturbation theory for $\mathcal{E}$ to the second order in field, Eq. (27a), is accurate up to $F \simeq 0.1$, 0.05, 0.05, and 0.03 for Ne($2p$), Ar($3p$), Kr($4p$), and Xe($5p$), respectively. These values of field correlate with the values of F_c estimated as the field where the WFAT(1) prediction for Γ turns zero and given by $F_c \simeq 0.3$, 0.12, 0.095, and 0.065, respectively. Similar to the case of H($1s$), Eq. (62) slightly overestimates the critical field giving $F_c \simeq 0.4$, 0.18,

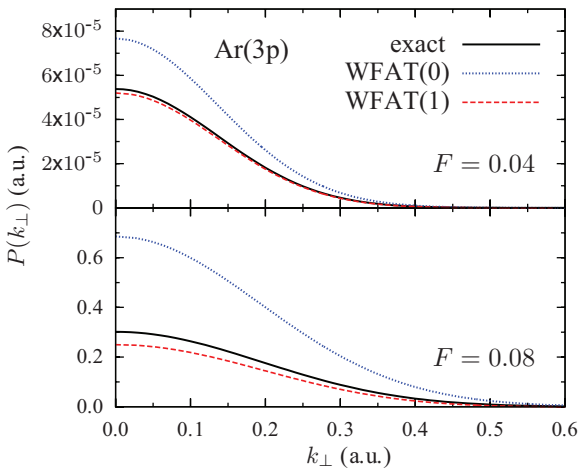

FIG. 9. (Color online) Same as in Fig. 8, but for Ar($3p$).

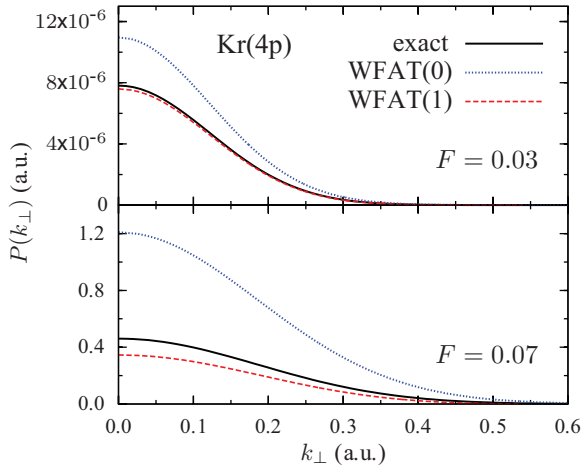

FIG. 10. (Color online) Same as in Fig. 8, but for Kr($4p$).

0.13, and 0.09, respectively. The exact results for the ratio shown in the bottom panels cannot be continued to smaller F because of a limitation of our double-precision calculations [14] discussed in Appendix B. However, even the available results unambiguously show that the WFAT(1) converges to the exact results as F decreases. This provides a numerical confirmation of Eq. (53) for non-Coulomb potentials, when Eqs. (12) are coupled in the core region $\eta < \eta_c$. We again conclude that for all atoms the first-order correction included in WFAT(1) significantly improves the results for Γ as compared to WFAT(0), extending the region of applicability of the theory up to $F \sim F_c$.

The results for the TMDs at two representative values of F for each of the atoms are shown in Figs. 8–11. The WFAT(0) and WFAT(1) results are obtained from Eq. (58) omitting and including the first-order correction terms (proportional to $F \ln F$ and F), respectively. Similar to the case of hydrogen illustrated in Fig. 3, the WFAT(1) prediction is always in much better agreement with the exact results than the WFAT(0), provided that the value of F is in the interval where Eq. (53) works well. This improvement of WFAT(1) over WFAT(0) is

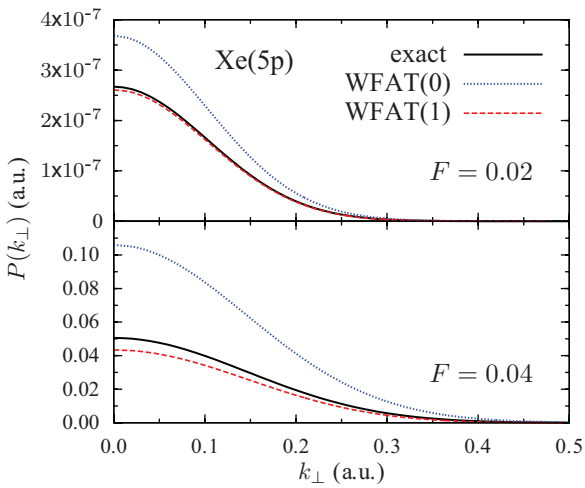

FIG. 11. (Color online) Same as in Fig. 8, but for Xe($5p$).

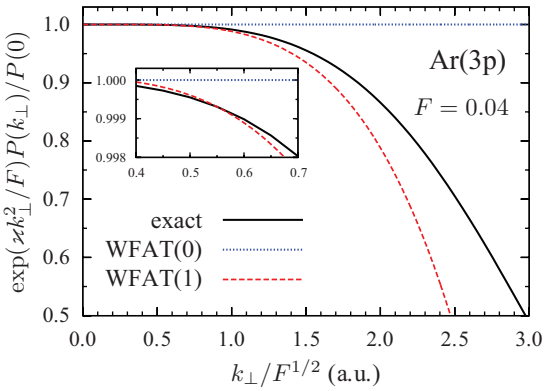

FIG. 12. (Color online) Transverse momentum distribution $P(k_\perp)$ for Ar($3p$) at $F = 0.04$ divided by the Gaussian distribution $P(0)\exp(-\varkappa k_\perp^2/F)$ as a function of the scaled transverse momentum. Solid (black) line: exact results. Dotted (blue) line, WFAT(0): the leading-order WFAT results. Dashed (red) line, WFAT(1): the WFAT results including the first-order correction.

again attributed to the s-independent part of the correction in Eq. (58).

Let us illustrate the role of the s-dependent part of the correction in Eq. (58), which accounts for a departure of the shape of the TMD from Gaussian, on the example of Ar($3p$). To facilitate the comparison of the different results, we divide the TMD $P(k_\perp)$ by $P(0)\exp(-\varkappa k_\perp^2/F)$. The results for this ratio as a function of the scaled transverse momentum $k_\perp/F^{1/2}$ are shown in Fig. 12. The field $F = 0.04$ considered coincides with that in the top panel of Fig. 9. The WFAT(1) is in much better agreement with the exact results than the WFAT(0), certainly qualitatively, but also quantitatively up to a certain value of the scaled momentum. For example, for the present case the error of the WFAT(1) does not exceed 10% up to $k_\perp/F^{1/2} = 2$, which corresponds to $k_\perp = 0.4$ in Fig. 9. This boundary value depends on field and decreases as F grows. Beyond this value the WFAT(1) quickly diverges from the exact results. All this agrees with a typical behavior of asymptotic expansions. As can be seen from Eqs. (22) and (23), the departure of the shape of the TMD from Gaussian results from two effects: the distortion of the eigenfunction for the dominant parabolic channel $\nu = (0,0)$ by field and the contribution from higher channels. In the weak-field limit, the first-order account of these effects is given by Eq. (58). As the field grows, the role of these effects also grows, and the TMD changes more considerably. In the over-the-barrier ionization regime the shape of the TMD may qualitatively differ from Gaussian [14].

V. CONCLUSIONS AND OUTLOOK

In this paper, the first-order correction terms in the asymptotic expansions of the ionization rate and TMD within the WFAT [16] are obtained. The results apply to any atom or molecule in a static electric field treated in the single-active-electron and frozen-nuclei approximations. So far, the first-order correction was available only for the ionization rate of hydrogen [24]. The present extension of these results in the analytical form to general atomic and molecular

potentials became possible on the basis of the method of Ref. [16], which takes the advantage of the separability of variables in the Schrödinger equation in parabolic coordinates in the asymptotic region, where the potential is dominated by the Coulomb tail. The illustrative calculations show that the inclusion of the first-order correction terms greatly improves the agreement between the rate and the TMD predicted by the WFAT and the results obtained from accurate numerical solution of the SS eigenvalue problem [14]. In practice, the present development extends the region of applicability of the WFAT at the quantitative level up to the boundary between tunneling and over-the-barrier regimes of ionization. Hence, the theory now covers a regime that has been notoriously difficult to describe by previous analytical approaches.

To evaluate the leading-order WFAT results [16], only the asymptotic charge Z and the energy E_0, dipole moment μ_z, and the asymptotic coefficient g_ν [Eq. (37)] for the dominant channel characterizing the unperturbed active orbital are needed. These characteristics define the structure (50) and field (51) factors. The techniques to calculate them for atoms and molecules based on quantum chemistry codes have been developed in Refs. [22,23]. To evaluate the first-order correction terms, one additionally needs the ionic dipole moment D_z, coefficients g_ν for several next-to-the-dominant channels, but also the polarizability α_{zz} and a new asymptotic coefficient a_ν [Eq. (38)] for the dominant channel which account for the second-order Stark shift and the distortion of the unperturbed orbital by field, respectively. These additional characteristics are needed to find the correction coefficients A_ν and B_ν, Eqs. (40). The calculation of α_{zz} and a_ν requires new techniques. The development of such techniques for general molecules using the experience gained in Refs. [22,23] is in progress.

In the present work the theory was demonstrated by calculations for atoms. The next goal is to extend its applications to molecules. It will, for example, be interesting to see whether the first-order correction to the ionization rate solves the controversies between theory and experiment for CO_2 [37,38], OCS [9], and CO [39] as to which orientation of the molecule with respect to the field produces maximum ionization yield.

ACKNOWLEDGMENTS

This work was supported by Grants-in-Aid for scientific research (B) and (C) from the Japan Society for the Promotion of Science, the Danish Natural Science Research Council, the Aarhus University Research Foundation, and an ERC-StG (Project No. 277767–TDMET). O.I.T. thanks the Russian Foundation for Basic Research for support through Grant No. 11-02-00390-a.

APPENDIX A: CONNECTION FORMULA

Here we consider an auxiliary problem, which gives the solution to Eq. (15) of the main text. Namely, we construct the asymptotics of the outgoing-wave solution of the equation

$$\left[\frac{d^2}{d\eta^2}+\frac{F\eta}{4}+\frac{E}{2}+\frac{\beta}{\eta}+\frac{\gamma}{\eta^2}\right]f(\eta)=0 \tag{A1}$$

for

$$F\to 0,\quad E=O(F^0),\quad \beta=O(F^0),\quad \gamma=O(F^0). \tag{A2}$$

The outer turning point for Eq. (A1) is given by

$$\eta_t=\frac{\kappa^2}{F}+O(F^0)=O(F^{-1}), \tag{A3}$$

where

$$\kappa=\sqrt{-2E}. \tag{A4}$$

Our goal is to derive the connection formula which expresses the coefficient of the outgoing wave at $\eta\gg\eta_t$ in terms of coefficients appearing in the expansion of the same solution at $1\ll\eta\ll\eta_t$.

1. Perturbation-theory solution in the inner region

We first consider Eq. (A1) in the inner region

$$1\ll\eta\ll F^{-1/2}. \tag{A5}$$

The term with F in this region can be treated perturbatively. For $F=0$, one of the two linearly independent solutions to Eq. (A1) behaves as

$$f_0(\eta)=\eta^{\beta/\kappa}e^{-\kappa\eta/2}\left[1+\frac{c_1}{\eta}+\frac{c_2}{\eta^2}+O(\eta^{-3})\right]. \tag{A6}$$

Substituting this expansion into Eq. (A1), we find

$$c_1=-\frac{\gamma}{\kappa}+\frac{\beta}{\kappa^2}-\frac{\beta^2}{\kappa^3}. \tag{A7}$$

The higher coefficients in Eq. (A6) can be found similarly. The second linearly independent solution diverges $\propto\eta^{-\beta/\kappa}e^{\kappa\eta/2}$ as η grows. In this case, the solution we need is given by

$$f(\eta)=gf_0(\eta), \tag{A8}$$

where g is a field-independent coefficient. For $F\neq 0$, the same solution is sought in the form

$$f(\eta)=g[f_0(\eta)+f_1(\eta)F+O(F^2)]. \tag{A9}$$

Substituting this into Eq. (A1) and neglecting terms $O(F^2)$, we obtain an inhomogeneous equation for $f_1(\eta)$,

$$\left[\frac{d^2}{d\eta^2}+\frac{E}{2}+\frac{\beta}{\eta}+\frac{\gamma}{\eta^2}\right]f_1(\eta)=-\frac{\eta}{4}f_0(\eta). \tag{A10}$$

The solution to this equation that decays as η grows can be sought in the form

$$f_1(\eta)=\eta^{\beta/\kappa}e^{-\kappa\eta/2}\left\{a_2\eta^2+a_1\eta+a_0+\frac{a_{-1}}{\eta}+O(\eta^{-2})+\left[b_0+\frac{b_{-1}}{\eta}+O(\eta^{-2})\right]\ln\eta\right\}. \tag{A11}$$

Substituting this expansion into Eq. (A10), we find

$$a_2=\frac{1}{8\kappa},\quad a_1=\frac{1}{4\kappa^2}\left(\frac{2-\gamma}{2}+\frac{5\beta}{2\kappa}-\frac{\beta^2}{2\kappa^2}\right), \tag{A12a}$$

$$b_0=\frac{1}{2\kappa^3}\left(\gamma+\frac{3\beta^2}{\kappa^2}\right). \tag{A12b}$$

One can continue and express a_{-1}, b_{-1}, and the higher coefficients in Eq. (A11) in terms of the coefficients in Eq. (A1)

and a_0. However, the coefficient a_0 cannot be found in this way. Such an uncertainty is explained by the fact that the solution to Eq. (A10) is defined up to an admixture of the solution $f_0(\eta)$ to the corresponding homogeneous equation. Summarizing,

$$f(\eta) = g\eta^{\beta/\kappa} e^{-\kappa\eta/2}\left\{1 - \left(\frac{\gamma}{\kappa} - \frac{\beta}{\kappa^2} + \frac{\beta^2}{\kappa^3}\right)\frac{1}{\eta} + O\left(\frac{1}{\eta^2}\right) + \left[\frac{\eta^2}{8\kappa} + \left(\frac{2-\gamma}{8\kappa^2} + \frac{5\beta}{8\kappa^3} - \frac{\beta^2}{8\kappa^4}\right)\eta + \left(\frac{\gamma}{2\kappa^3} + \frac{3\beta^2}{2\kappa^5}\right) \times \ln\eta + a_0 + O\left(\frac{\ln\eta}{\eta}\right)\right]F + O(F^2)\right\}. \quad \text{(A13)}$$

This is a perturbation-theory expansion in F for $F \to 0$ and asymptotic expansion in $1/\eta$ for $\eta \to \infty$. The terms $\propto 1/\eta$ and $\propto F$ within the curly brackets represent corrections existing without the field and caused by the field, respectively. The requirement that these terms must be much smaller than unity defines the lower and upper boundaries of the region of validity (A5) of this expansion. Note that these terms become comparable at $\eta = O(F^{-1/3})$, which belongs to the region (A5). The coefficients g and a_0 in Eq. (A13) remain undefined; they are determined by the behavior of $f(\eta)$ to the left of the region (A5), for example, by the regularity boundary condition at $\eta = 0$.

2. Asymptotic solution in the outer region

We now consider Eq. (A1) in the outer region

$$\eta = O(F^{-1}). \quad \text{(A14)}$$

Introducing a new variable,

$$y = \frac{F\eta}{\kappa^2} = O(F^0), \quad \text{(A15)}$$

we rewrite Eq. (A1) as

$$\left[\frac{d^2}{dy^2} + \frac{\kappa^4}{F^2}\,q(y)\right] f(y) = 0, \quad \text{(A16)}$$

where

$$q(y) = q_0(y) + q_1(y)F + q_2(y)F^2, \quad \text{(A17a)}$$

$$q_0(y) = \frac{\kappa^2}{4}(y-1), \quad q_1(y) = \frac{\beta}{\kappa^2 y}, \quad q_2(y) = \frac{\gamma}{\kappa^4 y^2}. \quad \text{(A17b)}$$

We seek the solution to Eq. (A16) in the form [27,28]

$$f(y) = f\exp\left\{\frac{i\kappa^2}{F}[s_0(y) + s_1(y)F + s_2(y)F^2 + s_3(y)F^3 + O(F^4)]\right\}, \quad \text{(A18)}$$

where f is a field-dependent coefficient. Substituting Eq. (A18) into Eq. (A16), we obtain equations defining $s_n(y)$,

$$-s_0'^2(y) + q_0(y) = 0, \quad \text{(A19a)}$$

$$-2s_0'(y)s_1'(y) + \frac{is_0''(y)}{\kappa^2} + q_1(y) = 0, \quad \text{(A19b)}$$

$$-s_1'^2(y) - 2s_0'(y)s_2'(y) + \frac{is_1''(y)}{\kappa^2} + q_2(y) = 0, \quad \text{(A19c)}$$

$$-2s_0'(y)s_3'(y) - 2s_1'(y)s_2'(y) + \frac{is_2''(y)}{\kappa^2} = 0. \quad \text{(A19d)}$$

The solutions to these equations are given by

$$s_0(y) = \frac{\kappa}{3}(y-1)^{3/2}, \quad \text{(A20a)}$$

$$s_1(y) = \frac{i}{4\kappa^2}\ln\frac{\kappa^2(y-1)}{4} + \frac{2\beta}{\kappa^3}\left[\arctan(y-1)^{1/2} - \frac{\pi}{2}\right], \quad \text{(A20b)}$$

$$s_2(y) = -\frac{5}{24\kappa^5(y-1)^{3/2}} + \frac{i\beta}{\kappa^6 y(y-1)} + \left[\frac{\gamma}{\kappa^5} + \frac{3\beta^2}{\kappa^7}\right] \times \frac{1}{(y-1)^{1/2}} - \left[\frac{\gamma}{\kappa^5} + \frac{\beta^2}{\kappa^7}\right]\frac{1}{y(y-1)^{1/2}} + \left[\frac{\gamma}{\kappa^5} + \frac{3\beta^2}{\kappa^7}\right]\left[\arctan(y-1)^{1/2} - \frac{\pi}{2}\right]. \quad \text{(A20c)}$$

The choice of the integration constants on the step from Eqs. (A19) to Eqs. (A20) is related to the definition of the coefficient f in Eq. (A18) and is dictated by the wish to arrive at Eq. (A22). The sign in Eq. (A20a) is determined by the outgoing-wave boundary condition. We have omitted the tedious expression for $s_3(y)$; in the following, we need this function only at $y \ll 1$ and $y \gg 1$, which can be easily obtained from Eq. (A19d) and the corresponding expansions for $s_0(y)$, $s_1(y)$, and $s_2(y)$ given below.

For $y \gg 1$, we have

$$s_0(y) = \frac{\kappa}{3}y^{3/2} - \frac{\kappa}{2}y^{1/2} + O(y^{-1/2}), \quad \text{(A21a)}$$

$$s_1(y) = \frac{i}{4\kappa^2}\ln\frac{\kappa^2 y}{4} + O(y^{-1/2}), \quad \text{(A21b)}$$

$$s_2(y) = O(y^{-1/2}), \quad s_3(y) = O(y^{-2}). \quad \text{(A21c)}$$

Thus

$$f(\eta)|_{\eta\gg\eta_t} = \frac{2^{1/2}f}{(F\eta)^{1/4}}\exp\left[\frac{iF^{1/2}\eta^{3/2}}{3} + \frac{iE\eta^{1/2}}{F^{1/2}}\right], \quad \text{(A22)}$$

which agrees with Eq. (17). For $y \ll 1$, we find

$$s_0(y) = -i\left[\frac{\kappa}{3} - \frac{\kappa y}{2} + \frac{\kappa y^2}{8} + O(y^3)\right], \quad \text{(A23a)}$$

$$s_1(y) = -i\left[\frac{\beta}{\kappa^3}\ln\frac{y}{4} - \frac{\ln(\kappa/2)}{2\kappa^2} - \frac{i\pi}{4\kappa^2} - \frac{i\pi\beta}{\kappa^3} + \left(\frac{1}{4\kappa^2} + \frac{\beta}{2\kappa^3}\right)y + O(y^2)\right], \quad \text{(A23b)}$$

$$s_2(y) = i\left[\frac{\gamma}{\kappa^5} - \frac{\beta}{\kappa^6} + \frac{\beta^2}{\kappa^7}\right]\frac{1}{y} - i\left[\frac{\gamma}{2\kappa^5} + \frac{3\beta^2}{2\kappa^7}\right]\ln\frac{y}{4} - i\left[\frac{5 + 12(1-i\pi)\gamma}{24\kappa^5} + \frac{\beta}{\kappa^6} + \frac{(5-3i\pi)\beta^2}{2\kappa^7}\right] + O(y^1), \quad \text{(A23c)}$$

$$s_3(y) = i\left[\frac{\gamma}{\kappa^5} - \frac{\beta}{\kappa^6} + \frac{\beta^2}{\kappa^7}\right]\left(\frac{\beta}{\kappa^4} - \frac{1}{\kappa^3}\right)\frac{1}{y^2} + O(y^{-1}). \quad \text{(A23d)}$$

Substituting these expansions into Eq. (A18) and considering the region (A5), where $y^2/F \ll 1$ and $F/y \ll 1$, we obtain

$$f(\eta) = f\,\exp\left[\frac{\kappa^3}{3F} - \frac{i\pi}{4} - \frac{i\pi\beta}{\kappa}\right]\sqrt{\frac{2}{\kappa}}\left(\frac{F\eta}{4\kappa^2}\right)^{\beta/\kappa} e^{-\kappa\eta/2}\left\{1 - \left(\frac{\gamma}{\kappa} - \frac{\beta}{\kappa^2} + \frac{\beta^2}{\kappa^3}\right)\frac{1}{\eta} + O\left(\frac{1}{\eta^2}\right) + \left[\frac{\eta^2}{8\kappa} + \left(\frac{2-\gamma}{8\kappa^2} + \frac{5\beta}{8\kappa^3} - \frac{\beta^2}{8\kappa^4}\right)\eta\right.\right.$$
$$+ \left(\frac{\gamma}{2\kappa^3} + \frac{3\beta^2}{2\kappa^5}\right)\ln\frac{F\eta}{4\kappa^2} + \left(\frac{10 + 18\gamma + 3\gamma^2}{48\kappa^3} + \frac{\beta(9-6\gamma)}{8\kappa^4} + \frac{\beta^2(49+2\gamma)}{16\kappa^5} - \frac{3\beta^3}{4\kappa^6} + \frac{\beta^4}{16\kappa^7}\right)$$
$$\left.\left. - i\pi\left(\frac{\gamma}{2\kappa^3} + \frac{3\beta^2}{2\kappa^5}\right) + O\left(\frac{\ln\eta}{\eta}\right)\right]F + O(F^2)\right\}. \tag{A24}$$

3. Matching

The inner, Eq. (A13), and outer, Eq. (A18), solutions can be matched in the region (A5), where they both apply. Indeed, expansions (A13) and (A24) have the same form. By comparing the coefficients in these expansions we find

$$f = g\,\exp\left[-\frac{\kappa^3}{3F} + \frac{i\pi}{4} + \frac{i\pi\beta}{\kappa}\right]\sqrt{\frac{\kappa}{2}}\left(\frac{4\kappa^2}{F}\right)^{\beta/\kappa}\left\{1 - \left[\left(\frac{\gamma}{2\kappa^3} + \frac{3\beta^2}{2\kappa^5}\right)\ln\frac{F}{4\kappa^2} + \frac{10 + 18\gamma + 3\gamma^2}{48\kappa^3}\right.\right.$$
$$\left.\left. + \frac{\beta(9-6\gamma)}{8\kappa^4} + \frac{\beta^2(49+2\gamma)}{16\kappa^5} - \frac{3\beta^3}{4\kappa^6} + \frac{\beta^4}{16\kappa^7} - a_0 - i\pi\left(\frac{\gamma}{2\kappa^3} + \frac{3\beta^2}{2\kappa^5}\right)\right]F + O(F^2)\right\}. \tag{A25}$$

This is the connection formula expressing the coefficient f in Eq. (A22) in terms of the field-independent coefficients g and a_0 appearing in Eq. (A13).

APPENDIX B: MULTIPLE-PRECISION NUMERICAL PROCEDURE FOR HYDROGEN

The ionization rate is determined by the imaginary part of the SS energy eigenvalue (18). In the weak-field limit (24) it becomes exponentially small, while the real part of the eigenvalue tends to a constant E_0. Therefore any numerical procedure of calculating Γ with finite-precision arithmetic fails at sufficiently small F, when the ratio $\Gamma/|E_0|$ approaches the value of the roundoff error. For neutral atoms in the ground state $|E_0| \sim 1$, so double-precision calculations [14] fail when $\Gamma \lesssim 10^{-12}$. This impedes extending the exact results shown in the bottom panels in Figs. 4–7 to smaller F. However, for hydrogen this fundamental problem can be overcome, at least in principle, for any nonzero F by using multiple-precision arithmetic [40,41]. We note that although there exist many efficient numerical techniques to calculate the ionization rate of hydrogen [42–50], the problem mentioned above, as far as we know, has never been addressed in the literature.

The peculiarity of hydrogen stems from the fact that the algorithm to calculate Γ can be formulated in a very simple form involving only basic arithmetic operations, which is required for the application of the multiple-precision package described in Refs. [40,41]. For $V(\mathbf{r}) = -1/r$, the variables in Eq. (1) can be separated in parabolic coordinates [17]. The solutions to the separated equations in ξ and η are then sought as expansions in a Laguerre basis similar to the one defined by Eq. (30b). To impose the outgoing-wave boundary condition (17) in such an L^2-integrable basis expansion approach, we rotate the ray $\eta \in [0,\infty)$ into the upper half of the complex plane by an angle $\sim\pi/3$ whose precise value for each state and field is found empirically. In this way the differential equations are turned into algebraic eigenvalue problems with five-diagonal symmetric matrices. The determinant of these matrices can be efficiently calculated by means of the recursive relations presented in Ref. [51]. For any given generally complex energy E, the eigenvalues of the equations in ξ and η can be found by the Newton-Raphson method [52]. The energy E is then adjusted to satisfy a relation for the eigenvalues [17]. The entire procedure can be relatively simply embedded in multiple-precision arithmetic [40] and works very fast. We thus could reproduce all significant digits in the available results for $\mathcal{E}$ and Γ obtained by other methods [42–50]. But the present procedure works also for very weak fields, when Γ attains extremely small values. The smallest F that can be treated is determined by the available computer memory. For example, with our computational resources we could obtain for the ground state $\Gamma = 0.694\,773\,113\,409\,051 \times 10^{-575}$ at $F = 5 \times 10^{-4}$, which is in full agreement with the WFAT(5) results [25].

[1] F. Krausz and M. Ivanov, Rev. Mod. Phys. **81**, 163 (2009).

[2] C. D. Lin, A.-T. Le, Z. Chen, T. Morishita, and R. Lucchese, J. Phys. B **43**, 122001 (2010).

[3] C. Wang, M. Okunishi, R. R. Lucchese, T. Morishita, O. I. Tolstikhin, L. B. Madsen, K. Shimada, D. Ding, and K. Ueda, J. Phys. B **45**, 131001 (2012).

[4] J. Maurer, D. Dimitrovski, L. Christensen, L. B. Madsen, and H. Stapelfeldt, Phys. Rev. Lett. **109**, 123001 (2012).

[5] T. Morishita, A.-T. Le, Z. Chen, and C. D. Lin, Phys. Rev. Lett. **100**, 013903 (2008).

[6] M. Uiberacker, T. Uphues, M. Schultze, A. J. Verhoef, V. Yakovlev, M. F. Kling, J. Rauschenberger, N. M. Kabachnik,

H. Schröder, M. Lezius, K. L. Kompa, H.-G. Muller, M. J. J. Vrakking, S. Hendel, U. Kleineberg, U. Heinzmann, M. Drescher, and F. Krausz, Nature (London) **446**, 627 (2008).

[7] L. Holmegaard, J. L. Hansen, L. Kalhoj, S. L. Kragh, H. Stapelfeldt, F. Filsinger, J. Küpper, G. Meijer, D. Dimitrovski, M. Abu-samha, C. P. J. Martiny, and L. B. Madsen, Nat. Phys. **6**, 428 (2010).

[8] A. N. Pfeiffer, C. Cirelli, M. Smolarski, D. Dimitrovski, M. Abu-samha, L. B. Madsen, and U. Keller, Natur. Phys. **8**, 76 (2012).

[9] J. L. Hansen, L. Holmegaard, J. H. Nielsen, H. Stapelfeldt, D. Dimitrovski, and L. B. Madsen, J. Phys. B **45**, 015101 (2012).

[10] J. Itatani, J. Levesque, D. Zeidler, H. Niikura, H. Pepin, J. Kieffer, P. Corkum, and D. Villeneuve, Nature (London) **432**, 867 (2004).

[11] H. Niikura, H. J. Wörner, D. M. Villeneuve, and P. B. Corkum, Phys. Rev. Lett. **107**, 093004 (2011).

[12] Y. Okajima, O. I. Tolstikhin, and T. Morishita, Phys. Rev. A **85**, 063406 (2012).

[13] O. I. Tolstikhin and T. Morishita, Phys. Rev. A **86**, 043417 (2012).

[14] P. A. Batishchev, O. I. Tolstikhin, and T. Morishita, Phys. Rev. A **82**, 023416 (2010).

[15] L. Hamonou, T. Morishita, and O. I. Tolstikhin, Phys. Rev. A **86**, 013412 (2012).

[16] O. I. Tolstikhin, T. Morishita, and L. B. Madsen, Phys. Rev. A **84**, 053423 (2011).

[17] L. D. Landau and E. M. Lifshitz, *Quantum Mechanics (Non-Relativistic Theory)* (Pergamon Press, Oxford, 1977).

[18] S. Yu. Slavyanov, Probl. Mat. Fiz. No. 4, 125 (1970) [English translation: *Topics in Mathematical Physics* (Consultants Bureau, New York, London, 1971), Vol. 4].

[19] T. Yamabe, A. Tachibana, and H. J. Silverstone, Phys. Rev. A **16**, 877 (1977).

[20] B. M. Smirnov and M. I. Chibisov, Zh. Eksp. Teor. Fiz. **49**, 841 (1965) [Sov. Phys.-JETP **22**, 585 (1966)].

[21] O. I. Tolstikhin, H. J. Wörner, and T. Morishita, Phys. Rev. A **87**, 041401(R) (2013).

[22] L. B. Madsen, O. I. Tolstikhin, and T. Morishita, Phys. Rev. A **85**, 053404 (2012).

[23] L. B. Madsen, F. Jensen, O. I. Tolstikhin, and T. Morishita, Phys. Rev. A **87**, 013406 (2013).

[24] R. J. Damburg and V. V. Kolosov, J. Phys. B **11**, 1921 (1978); **12**, 2637 (1979).

[25] H. J. Silverstone, E. Harrell, and C. Grot, Phys. Rev. A **24**, 1925 (1981).

[26] *Handbook of Mathematical Functions*, edited by M. Abramowitz and I. A. Stegun (Dover, New York, 1972).

[27] F. W. J. Olver, *Asymptotics and Special Functions* (Academic Press, New York, 1974).

[28] M. V. Fedoryuk, *Asymptotic Analysis: Linear Ordinary Differential Equations* (Springer-Verlag, Berlin, 1993).

[29] A. I. Nikishov and V. I. Ritus, Zh. Eksp. Teor. Fiz. **50**, 255 (1966) [Sov. Phys.-JETP **23**, 162 (1966)].

[30] A. M. Perelomov, V. S. Popov, and M. V. Terent'ev, Zh. Eksp. Teor. Fiz. **50**, 1393 (1966) [Sov. Phys.-JETP **23**, 924 (1966)]; Zh. Eksp. Teor. Fiz. **51**, 309 (1966) [Sov. Phys.-JETP **24**, 207 (1967)].

[31] N. B. Delone and V. P. Krainov, J. Opt. Soc. Am. B **8**, 1207 (1991).

[32] C. Bracher, W. Becker, S. A. Gurvitz, M. Kleber, and M. S. Marinov, Am. J. Phys. **66**, 38 (1998).

[33] H. J. Silverstone, Phys. Rev. A **18**, 1858 (1978).

[34] A. E. S. Green, D. L. Sellin, and A. S. Zachor, Phys. Rev. **184**, 1 (1969).

[35] R. H. Garvey, C. H. Jackman, and A. E. S. Green, Phys. Rev. A **12**, 1144 (1975).

[36] O. I. Tolstikhin and C. Namba, *CTBC—A Program to Solve the Collinear Three-Body Coulomb Problem: Bound States and Scattering Below the Three-Body Disintegration Threshold, Research Report NIFS-779* (National Institute for Fusion Science, Toki, Japan, 2003) [http://www.nifs.ac.jp/report/nifs779.html].

[37] D. Pavičić, K. F. Lee, D. M. Rayner, P. B. Corkum, and D. M. Villeneuve, Phys. Rev. Lett. **98**, 243001 (2007).

[38] I. Thomann, R. Lock, V. Sharma, E. Gagnon, S. T. Pratt, H. C. Kapteyn, M. M. Murnane, and W. Li, J. Phys. Chem. A **112**, 9382 (2008).

[39] J. Wu, L. P. H. Schmidt, M. Kunitski, M. Meckel, S. Voss, H. Sann, H. Kim, T. Jahnke, A. Czasch, and R. Dörner, Phys. Rev. Lett. **108**, 183001 (2012).

[40] D. M. Smith, Comput. Sci. Eng. **5**, 88 (2003).

[41] See http://myweb.lmu.edu/dmsmith/FMLIB.html.

[42] M. H. Alexander, Phys. Rev. **178**, 34 (1969).

[43] M. Hehenberger, H. V. McIntosh, and E. Brändas, Phys. Rev. A **10**, 1494 (1974).

[44] N. A. Guschina and V. K. Nikulin, Chem. Phys. **10**, 23 (1975).

[45] R. J. Damburg and V. V. Kolosov, J. Phys. B **9**, 3149 (1976).

[46] H. J. Silverstone, B. G. Adams, J. Cizek, and P. Otto, Phys. Rev. Lett. **43**, 1498 (1979).

[47] L. Benassi and V. Grecchi, J. Phys. B **13**, 911 (1980).

[48] A. Maquet, Shih-I. Chu, and W. P. Reinhardt, Phys. Rev. A **27**, 2946 (1983).

[49] V. Franceschini, V. Grecchi, and H. J. Silverstone, Phys. Rev. A **32**, 1338 (1985).

[50] C. A. Nicolaides and S. I. Themelis, Phys. Rev. A **45**, 349 (1992).

[51] I. Kátai and E. Rahmy, Ann. Univ. Sci. Budap. Rolando Eötvös, Sect. Comput. **2**, 13 (1979).

[52] W. H. Press, S. A. Teukolsky, W. T. Vetterling, and B. P. Flannery, *Numerical Recipes in FORTRAN* (Cambridge University Press, Cambridge, 1992).